Proceedings of ISFOG 2025
5TH INTERNATIONAL SYMPOSIUM ON
FRONTIERS IN OFFSHORE GEOTECHNICS
Nantes, France | June 9-13 2025

ISBN 978-2-85782-758-0

Simplified calculation of wave-induced accumulated damage zone in clayey seabeds for gravity-based foundation

H.L. Chen
Shanghai Jiao Tong University, Shanghai, China

L.L. Zhang*, C.C. Liao
Shanghai Jiao Tong University, Shanghai, China

**lulu_zhang@sjtu.edu.cn (corresponding author)*

ABSTRACT: Clayey seabeds are susceptible to damage due to wave action, which limits the number of cycles they can endure. The number of cycles experienced up to the limit indicates the level of soil damage. Identifying the damage zone is crucial for assessing potential failure risks, such as settlement or sliding, in gravity-based foundations during storm events. This paper proposes a simplified, explicit method for the calculation of damage zone, allowing for rapid analysis over a large number of cycles. The method requires only the shear stress-strain relationship, which is derived from cyclic shear tests, to assess the damage of soil elements. Along with a simple finite element program to obtain the stress field, it can be easily extended to the damage zone in seabed soil. By quantifying changes in the damaged area, this method efficiently evaluates the stability of foundation. From the perspective of soil damage, this paper expends the application of the equivalent number of cycles for simplified assessment of potential failure risk in gravity-based foundation. Additionally, this approach avoids simulation accuracy issues arising from complex dynamic calculation.

Keywords: Wave loads; Clayey seabed; Damage zone; Gravity-based foundation.

1 INTRODUCTION

Numerous field and laboratory tests show that the elastoplastic behaviour of soil under cyclic loading differs from that under monotonic loading. The shear stiffness and strength will gradually reduce with increasing cycles, indicating a trend of weakening in clayey seabeds. This trend will lead to the development of soil damage. Therefore, it is essential to assess the level of accumulated damage and calculate the damage zone in clayey seabeds.

To better simulate the cyclic response of clayey seabeds, researchers have developed numerous soil constitutive models based on theoretical analyses and experimental tests. For example, Cheng et al. (2016) established an elastoplastic boundary layer model to characterise the weakening of clayey soil strength. Zhang et al. (2023) presented a cyclic-softening macro element model to capture the softening behaviour of foundation subjected to a load sequence through the contraction of yield surfaces. The majority of these models hinge on traditional constitutive models, and incorporate the cyclic behaviour of soil into their calculations. While they can accurately capture the soil deformations, there exist comparatively few models that calculate the soil damage in a simple and efficient way.

Over the past 40 years, NGI has developed a framework based on the concept of equivalent number of cycles to describe the soil dynamic behaviour (Andersen et al., 1988; Andersen, 2009). Combined with the shear stress-strain relationship from cyclic shear tests and limiting equilibrium stability computer program, the framework worked well in the analysis of marine foundation stability (Keaveny et al., 1994; Jostad et al., 2015). NGI further developed a finite element program, UDCAM, to calculate the accumulated shear strain in soil and later introduced a simplified version (Jostad et al., 2014, 2023). In order to determine the bearing capacity of the foundation, these models mentioned above typically calculate the post-cyclic shear strength after reaching the equivalent number of cycles. This involves scaling the cyclic strength until the soil's resistance equilibrates with the applied peak loads. However, the process of calculating the equivalent number of cycles incorporates geotechnical characteristics of the cyclic behaviour. Instead of directly calculating the cyclic shear strength, the equivalent number of cycles can be expended to define a damage index for the soil. This index helps us map out areas where the soil might be weakened, and can be readily extended to assess the potential failure risk of marine gravity-based foundations.

Based on the concept of equivalent number of cycles, this paper further defines damage index for soil elements. Additionally, the paper proposes a straightforward method for calculating the distribution of the damage zone, and its variation in area can be used to assess the stability of the seabed soil. In this paper, a case study of a gravity-based foundation is presented to illustrate the proposed calculation of damage zone in seabed soil.

2 CALCULATION METHODS

2.1 Cyclic load composition

This paper uses load parcels to characterize irregular load history. This transformation avoids the accuracy issues associated with many cycles. The rain-flow is one of typically algorithms used to address this transformation. The effects of other algorithms on the soil's cyclic dynamic response can be found in Norén-Cosgriff et al. (2015). Figure 1 illustrates this transformation process. It can be found that the average wave load (F_a) is typically a constant value, while the cyclic load (F_{cy}) varies with corresponding number of cycles (N). Accordingly, the load history is transformed into several regular load parcels.

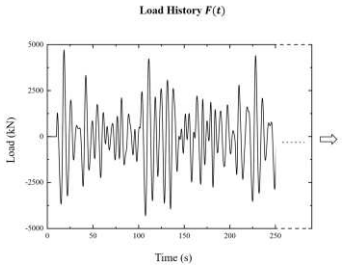

Load Parcel ($F_a + F_{cy}$, N)

Parcel Order	Number of Cycles, N	Average Load Amplitude, F_a	Cyclic Load Amplitude, F_{cy}
9	1	400 kN	4000 kN
8	3	400 kN	3560 kN
7	10	400 kN	3000 kN
6	25	400 kN	2480 kN
5	64	400 kN	2040 kN
4	163	400 kN	1600 kN
3	1079	400 kN	1040 kN
2	2877	400 kN	440 kN
1	2371	400 kN	80 kN

Figure 1. Transformation of load history (only part of load history is shown) to load parcels.

2.2 Undrained cyclic behaviour of clay

In undrained cyclic shear tests, the shear stress of soil consists of two components: average shear stress (τ_a) and cyclic shear stress (τ_{cy}). The average shear stress is composed of the initial shear stress generated by the weight of the soil and the additional shear stress produced by the weight of the structure. The cyclic shear stress is generated by the cyclic dynamic loads. In particle engineering, the average shear stress usually remains constant. The relationship between average (τ_a) and cyclic shear stress (τ_{cy}) can be clearly illustrated in Figure 2.

The shear strain of soil can also be divided into two components: average shear strain (γ_a) and cyclic shear strain (γ_{cy}). Both will be affected by the combination of shear stresses (τ_a, τ_{cy}). In undrained cyclic shear tests, average and cyclic shear strain will gradually accumulate with the increase of the number of cycles (N). Figure 2 show the development of average and cyclic shear strains with increasing number of cycles.

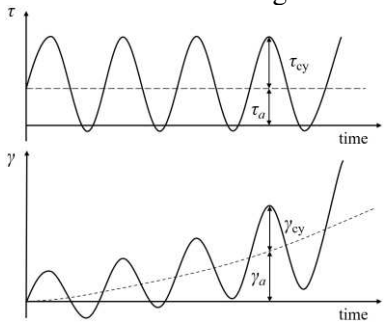

Figure 2. Development of average and cyclic shear strains with increasing number of cycles in a soil element subjected to combined average and cyclic shear stresses.

The relationship between shear stress and shear strain can be expressed using the following equations:

$$\gamma_a = \gamma_a(\tau_a, \tau_{cy}, N) \quad (1)$$

$$\gamma_{cy} = \gamma_{cy}(\tau_a, \tau_{cy}, N) \quad (2)$$

The relation among shear strain, shear stress and the number of cycles can be depicted by shear strain contour diagrams (Figure 3). To simplify, one shear stress is assumed to be known (fixed value). Both average and cyclic shear stress are normalized by undrained shear strength (S_u), allowing shear strain to be calculated based on the number of cycles and the normalized shear stresses.

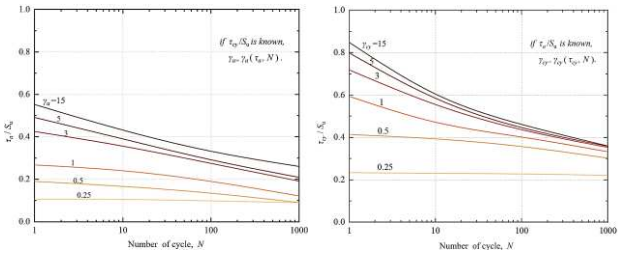

(a) *(b)*

Figure 3. Shear strain contour diagrams. (a) Average shear strain. (b) Cyclic shear strain.

2.3 Accumulated damage for soil elements

Andersen (2015) pointed out that the accumulated shear strain can be used to describe the effects of cyclic loading. Figure 4 illustrates the accumulation of average and cyclic shear strain, respectively. Take the average shear strain as example (Figure 4(a)). A_1-B_1 represents the cyclic loading process with the first load parcel. Average shear strain (γ_a) can be obtained by the normalized shear stresses (τ_a/S_u, τ_{cy}/S_u) and the

number of cycles (N). The B_1-A_1 is the prepararion process before the second load parcel. By keeping the shear strain constant, the number of cycles corresponding to the current stress level (first parcel) is converted into the equivalent number of cycles for the next stress level (second parcel). This method allows for the nonlinear superposition of the number of cycles from different stress levels. Thus, A_2-B_2 is the cylic loading process of the second load parcel, subsequent to the first. Through further iterations (A_1-B_1-A_2-B_2-A_3-B_3), the final accumulated average shear strain from three load parcels can be obtained.

The endpoint of the final iteration is labeled B_n (point B_3 in Figure 4(a)). Its horizontal coordinate represents the final equivalent number of cycles (N_{eq}). At the maximum stress level, there is a number of cycle where the calculated shear strain reaches 15 % (point C in Figure 4(a)). This strain indicates that the soil has completely failed (Andersen, 2015). Therefore, this number is defined as the maximum number of cycles (N_{max}). In the field of metal fatigue, the ratio of the number of cycles experienced up to the maximum the material can withstand, is often used to assess the degree of damage. Therefore, this study defines the ratio of the soil's final equivalent number of cycle (N_{eq}) to the maximum number (N_{max}) as the damage index (D):

$$D = N_{eq}/N_{max} \tag{5}$$

The damage calculated from the average shear strain contour diagram (Figure 4(a)) is denoted as D_1, and the damage calculated from the cyclic shear strain contour diagram (Figure 4(b)) is denoted as D_2.

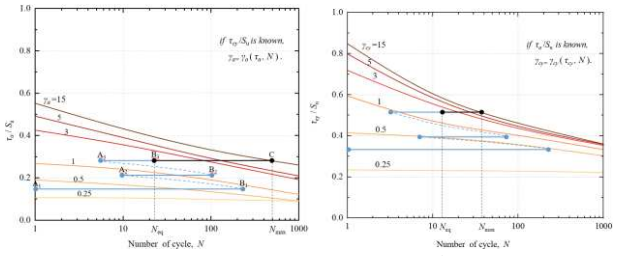

(a) *(b)*

Figure 4. The accumulation of shear strain and the definition of damage index for soil element. (a) average shear strain; (b) cyclic shear strain

2.4 Accumulated damage zone in seabed soil

To obtain the accumulated damage zone, it is necessary to determine the shear stress field in the soil, specifically the average and cyclic shear stress fields. Both can be obtained using finite element programs. The average shear stress field is derived from the self-weight of the soil and the marine structure; the cyclic shear stress field is calculated based on cyclic loading amplitude. It should be noted that this is not a dynamic calculation but rather a static calculation.

However, the finite element calculation result is the stress state of the integration point, which is not the same as the shear stress applied in soil tests. Therefore, it is necessary to establish the stress relationship between the integration point and the soil tests. Jostad et al. (2014) utilized the anisotropic shear strength model to describe this relationship. The model introduced an equivalent isotropic shear stress (τ), which is derived from three shear stresses in DSS tests (τ_{DSS}) and dynamic triaxial tests (τ_C and τ_E) corresponding to the equivalent shear strain (γ_{eq}). Meanwhile, the equivalent isotropic shear stress can also be derived from the principal deviatoric stresses. Thus, the stress relationship is established between the integration point and the soil tests. In this paper, it is assumed that the shear stress in the DSS tests (τ_{DSS}) could represent equivalent isotropic shear stress (τ). This approximation is acceptable, as there is a detailed discussion of this issue from the perspectives of shear strength, stress-strain behaviour, and foundation bearing capacity (Andersen, 2015; Rasch, 2016).

Figure 5 shows the calculation process of accumulated damage zone in seabed soil.

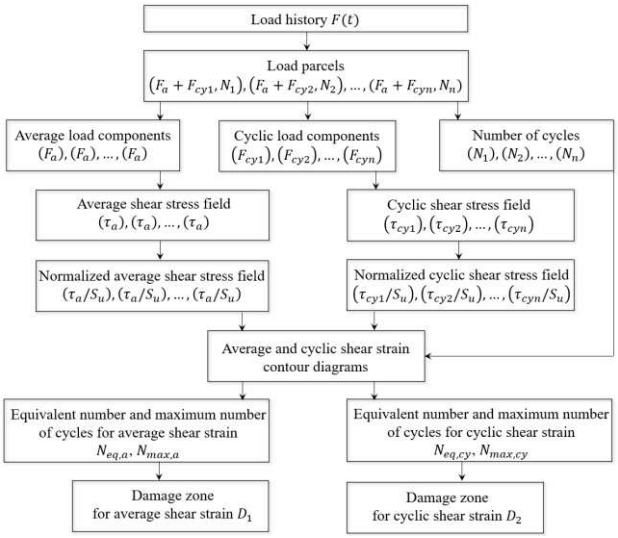

Figure 5. The calculation process of accumulated damage zone in seabed soil

3 CASE STUDY

A marine fish cage (Figure 6) is served as the subject in the case study. The width of gravity-based foundation is 20 m. The load parcels applied in the case study are illustrated in Figure 7. In this case, the shear stress-strain relationship is initially used to determine the damage zone in seabed soil. Then, the rapid increase in the damaged area indicates the seabed

soil is is in a stage with a high potential for failure. Finally, the influence of the OCR on the distribution of damage in seabed soil is explored.

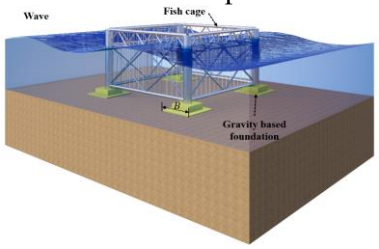

Figure 6. Marine fish cage with gravity-based foundation

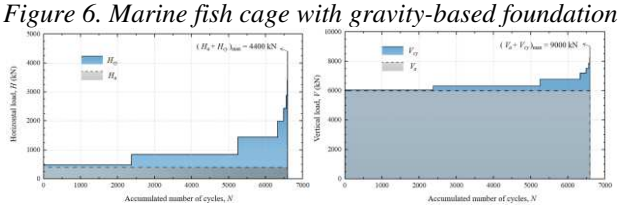

(a) Horizontal load parcels (b) Vertical load parcels
Figure 7. The load parcels applied in the case study.

The soil properties used in this study are derived from Drammen Clay, for which NGI has performed numerous dynamic shear tests. Figure 8 and Figure 9 show the shear stress-strain relationship for soil with OCR = 1. For average shear strain, its accumulated results are closely related to cyclic shear stress. Therefore, the average shear strain contour diagrams (Figure 8) corresponds to different normalized cyclic shear stresses (τ_{cy}/S_u = 0, 0.1, 0.2, 0.3, 0.4, 0.5). For cyclic shear strain, its accumulated results are little affected by the average shear stress. Therefore, the cyclic shear strain contour diagram (Figure 9) encompasses various average shear stress (τ_a/S_u = 0~1). It is important to note that this phenomenon is specific to Drammen Clay and does not imply similar results for other types of soil.

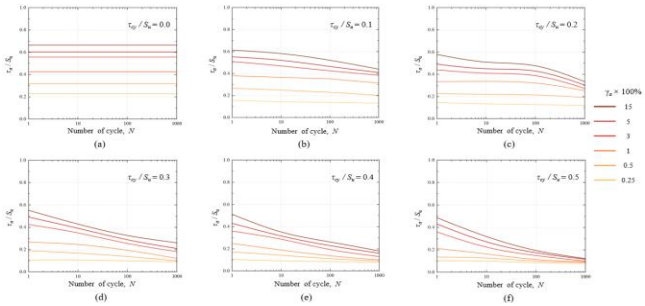

Figure 8. Average shear strain contour diagrams

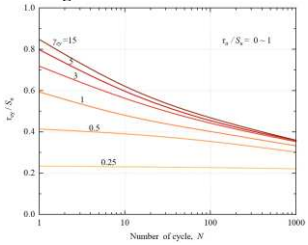

Figure 9. Cyclic shear strain contour diagram

Figure 10 illustrates the variation in damage zone with the increase in cyclic loads. The study selects different scaling ratios (1.0, 1.4, 1.8) to simulate the amplification of cyclic loads (H_{cy}, V_{cy}). The damage zone on the left side is based on average shear strain (D_1), while the damage zone on the right side is based on cyclic shear strain (D_2). Figure 10 illustrates that as the cyclic load increases, both the average and cyclic damage zone of the soil gradually expand. Damage zone of D_1 is concentrated at the edges of the foundation, while The distribution of D_2 at the base is more uniform. This is because the average load is mainly vertical, whereas the cyclic load is primilary horizontal.

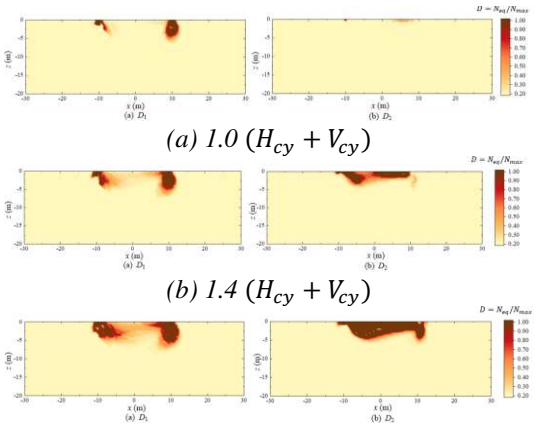

(a) 1.0 ($H_{cy} + V_{cy}$)

(b) 1.4 ($H_{cy} + V_{cy}$)

(c) 1.8 ($H_{cy} + V_{cy}$)

Figure 10. The damage zone expands with the increase in cyclic load for different scaling ratios.
(Left is D_1, defined by average shear strain;
Right is D_2, defined by cyclic shear strain).

Figure 11 is derived from the damage zone in Figure 10. It shows the change in the percentage of the complete damage zone area ($D > 1$) and little affected damage zone area ($D < 0.01$) compared to the affected zone area with the increase in scaling ratio of cyclic load. The damage zone where the damage index exceeds 1 indicates that the soil is in a plastic flow state and has lost its strength. Conversely, the damage zone where the damage index is less than 0.01 indicates that the soil is little affected by cyclic loading. The affected zone is defined as having a depth equal to foundation's width and a width extending 1.5 times the foundation's width on both sides of the center.

Figure 11 shows that as cyclic load (F_{cy}, the combination of H_{cy} and V_{cy}) increases, the areas of the average and cyclic complete damage zones (red curves) increase, with inflection points occurring at $1.2F_{cy}$ for cyclic (circle) and $1.6F_{cy}$ for average (square). Meanwhile, the areas of the average and cyclic little affected damage zones (black curves) decrease, with inflection points occurring at $1.2F_{cy}$ for cyclic (circle) and $1.6F_{cy}$ for average (square). This

indicates faster development of cyclic damage. Therefore, D_1 can be used as the stability control index for seabed soil, and $1.2F_{cy}$ as the maximum cyclic load for the foundation design.

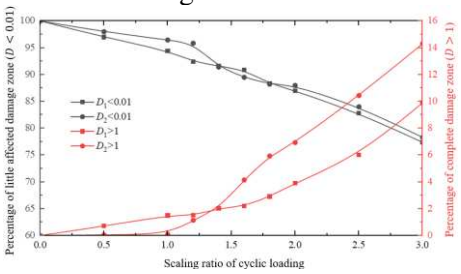

Figure 11. The change in the percentage area of damage zone with the increase in cyclic loading (F_{cy}).

This paper explores the effect of soil with different OCR. Figure 12 and Figure 13 illustrates the average and cyclic shear strain contour diagrams for different OCR (OCR = 1, 4). Each contour diagram is composed of a cluster of six average shear strain curves (γ_{cy} = 0.25 %, 0.5 %, 1 %, 3 % %, 5 %, 15 %). The slope of the cluster indicates the rate at which soil strength decreases with the increasing of cycles. Figure 12 and Figure 13 show that the slope of the shear strain cluster, changes from fast to slow in the following order: OCR = 4, 1. This indicates that soil strength weakening is more sensitive at higher OCR. This may be because soils with a higher OCR have stronger structural integrity, which can be easily damaged by cyclic load.

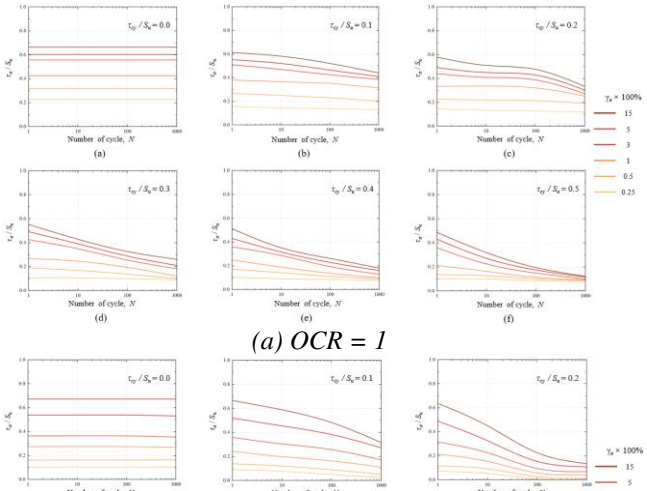

(a) OCR = 1

(b) OCR = 4

Figure 12. Average shear strain contour diagrams for different OCR.

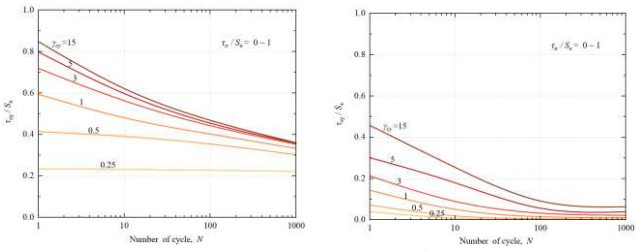

(a) OCR = 1 *(b) OCR = 4*

Figure 13. Cyclic shear strain contour diagrams for different OCR.

Figure 14 illustrates the damage zone in clayey seabed at different OCR with the same vertical effective stress. It reveals that a higher OCR results in increased static undrained strength of the soil. However, a higher OCR makes the soil more susceptible to cyclic load. Figure 15 indicates that for soils with the same undrained shear strength, those with a higher OCR are more prone to be damaged.

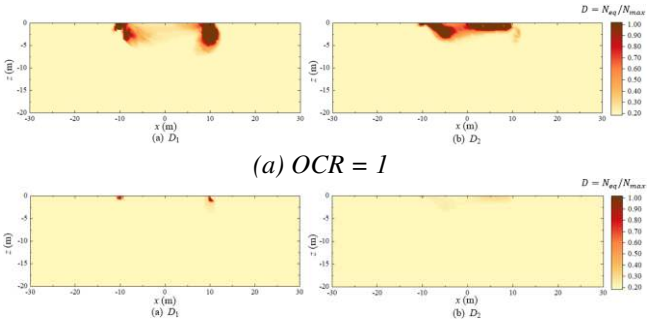

(a) OCR = 1

(b) OCR = 4

Figure 14. Accumulated damage zone with different OCRs obtained under the same vertical effective stress.

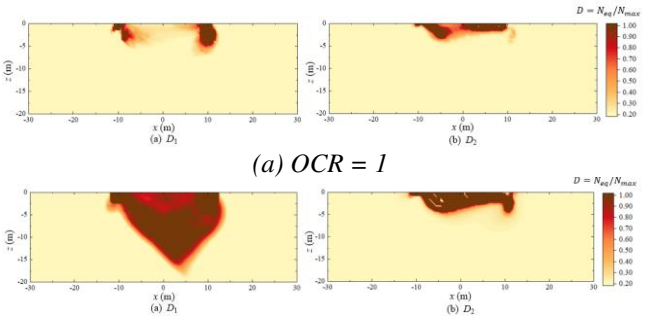

(a) OCR = 1

(b) OCR = 4

Figure 15. Accumulated damage zone with different OCR obtained under the same undrained shear strength.

4 CONCLUSIONS

This study proposed a straightforward method to evaluate the potential failure risk of gravity-based foundations caused by cyclic wave action, through quantifying the damage zone in clayey seabeds. The method utilizes shear strain contour diagrams to characterize the relationship between shear strain, shear stress and the numbers of cycles. This paper

extended the process of shear strain accumulation to the damage index, and provided a simplified, explicit method for the calculation of damage zone. By analysing changes in the size of this damaged area, the method provides an effective way to assess the stability of gravity-based foundations. The article also discussed the impact of over consolidated ratio of soil, finding that a larger OCR makes soil strength more susceptible to cyclic loading. A limitation of this method is that the contour diagrams depend on the soil's characteristics, meaning that a few dynamic shear tests are required for new sites. Future research could focus on investigating the dynamic behaviour of contour diagrams for various soil types, as well as establish safety evaluation standards based on the extent of damage observed in seabed soil.

AUTHOR CONTRIBUTION STATEMENT

H.L. Chen: Conceptualization, Methodology, Formal analysis, Writing – original draft. **L.L. Zhang**: Resources, Supervision, Project, administration, Funding acquisition. **C.C. Liao:** Software, Writing, – review & editing.

ACKNOWLEDGEMENTS

The work in this paper was supported by the Scientific Research and Innovation Plan of Shanghai Municipal Education Commission (Grant No.2021-01-07-00-02-E00089), the Natural Science Foundation of China (Grant No. 52025094 and 52279106).

REFERENCES

Andersen, K. H., Kleven, A., & Heien, D. (1988). Cyclic soil data for design of gravity structures. *Journal of Geotechnical engineering*, 114(5), 517-539.

Andersen, K. H. (2009). Bearing capacity under cyclic loading—offshore, along the coast, and on land. The 21st Bjerrum Lecture presented in Oslo, 23 November 2007. *Canadian Geotechnical Journal*, 46(5), 513-535.

Andersen, K. H. (2015). Cyclic soil parameters for offshore foundation design, In *Frontiers in offshore geotechnics III*, Vaughan Meyer (eds.), pp. 5-82. Leiden: Taylor & Francis Books Ltd.

Cheng, X., & Wang, J. (2016). An elastoplastic bounding surface model for the cyclic undrained behaviour of saturated soft clays. *Geomechanics & engineering*, 11(3), 325-343.

Jostad, H. P., Grimstad, G., Andersen, K. H., Saue, M., Shin, Y., & You, D. (2014). A FE procedure for foundation design of offshore structures–applied to study a potential OWT monopile foundation in the Korean Western Sea. *Geotechnical Engineering Journal of the SEAGS & AGSSEA*, 45(4), 63-72.

Jostad, H., Torgersrud, Ø., and Engin, H. (2015). A FE procedure for calculation of fixity of jack-up foundations with skirts using cyclic strain contour diagrams. *The 15th International Conference: The Jack-up Platform*, London, United Kingdom.

Jostad, H. P., Liu, H., & Sivasithamparam, N. (2023). Accounting for effects of cyclic loading in design of offshore wind turbine foundations. *10th European Conference on Numerical Methods in Geotechnical Engineering*, London, United Kingdom.

Keaveny, J. M., Hansen, S. B., Madshus, C., & Dyvik, R. (1994). Horizontal capacity of large-scale model anchors. *In International conference on soil mechanics and foundation engineering* (pp. 677-680).

Norén-Cosgriff, K., Jostad, H. P., & Madshus, C. (2015). Idealized load composition for determination of cyclic undrained degradation of soils. *Frontiers in Offshore Geotechnics III: Proceedings of the 3rd International Symposium on Frontiers in Offshore Geotechnics* (Vol. 1, pp. 1097-1102). Taylor & Francis Books Ltd.

Rasch, C. (2016). *Modelling of cyclic soil degradation: Development of a cyclic accumulation model and the application to a gravity-based foundation*. Master's Thesis, Delft University of Technology, Delft, The Netherlands, 201

Zhang, C., Wang, D., & Zheng, J. (2023). A cyclic-softening macro element model for mono-bucket foundations supporting offshore wind turbines in clay. *Computers and Geotechnics*, 161, 105603.